Recurrent epidemics in small world networks

J. Verdasca[a], M.M. Telo da Gama[a,*], A. Nunes[a], N.R. Bernardino[a],
J.M. Pacheco[a], M.C. Gomes[b]

[a]*Centro de Física Teórica e Computacional and Departamento de Física, Faculdade de Ciências da Universidade de Lisboa,
Avenida Professor Gama Pinto 2, P-1649-003 Lisboa Codex, Portugal*
[b]*Departamento de Biologia Vegetal, Faculdade de Ciências da Universidade de Lisboa, Campo Grande, 1749-016 Lisboa, Portugal*

Abstract

The effect of spatial correlations on the spread of infectious diseases was investigated using a stochastic susceptible-infective-recovered (SIR) model on complex networks. It was found that in addition to the reduction of the effective transmission rate, through the screening of infectives, spatial correlations have another major effect through the enhancement of stochastic fluctuations, which may become considerably larger than in the homogeneously mixed stochastic model. As a consequence, in finite spatially structured populations significant differences from the solutions of deterministic models are to be expected, since sizes even larger than those found for homogeneously mixed stochastic models are required for the effects of fluctuations to be negligible. Furthermore, time series of the (unforced) model provide patterns of recurrent epidemics with slightly irregular periods and realistic amplitudes, suggesting that stochastic models together with complex networks of contacts may be sufficient to describe the long-term dynamics of some diseases. The spatial effects were analysed quantitatively by modelling measles and pertussis, using a susceptible-exposed-infective-recovered (SEIR) model. Both the period and the spatial coherence of the epidemic peaks of pertussis are well described by the unforced model for realistic values of the parameters.
© 2004 Elsevier Ltd. All rights reserved.

Keywords: Epidemiology; Spatial structure; Complex networks; Recurrent epidemics

1. Introduction

Deterministic models of epidemic spread have been used for decades and developed into a mature branch of applied mathematics. Indeed these models proved successful in understanding some of the mechanisms determining the time evolution and the spread of a variety of infectious diseases, spawning the development of strategies of epidemic control (Anderson and May, 1991; Hethcote, 2000; Murray, 2003). When applied to immune-for-life diseases such as measles, these models account for the observed undamped oscillations registered in the pre-vaccination era through the introduction

of seasonal forcing terms (Aron and Schwartz, 1984; Bolker, 1993; Dietz, 1976; Keeling and Grenfell, 1997, 2002). Indeed, the seasonally forced susceptible-infective-recovered (SIR) model describes the pre-vaccination data for measles semi-quantitatively, due to the prominence of epidemic annual/biennial cycles, corresponding to moderate annual forcing (Earn et al., 2000).

Nevertheless, the importance of demographic stochasticity in the dynamics and persistence of childhood diseases has long been acknowledged, not in the least because of stochastic extinction. In the work published in the 1950s, Bartlett (Bailey, 1975; Bartlett, 1957) has shown how a stochastic version of the deterministic SIR model exhibits small amplitude fluctuations, modulated by the underlying deterministic period. In the linear regime, for sufficiently large populations, these fluctuations are Gaussian and scale as the square root of the

population size (Bailey, 1975), while for smaller population sizes the relative fluctuations are larger and may lead to stochastic extinction (Anderson and May, 1986; Bartlett, 1957). More recently, several authors have stressed the need for realistic models, both forced and unforced, to include stochastic effects (Aparicio and Solari, 2001; Nåsell, 1999; Rohani et al., 1999, 2002) in order to describe various aspects of incidence time series, such as the observed different patterns of recurrent epidemics. A more systematic treatment of the shortcomings of deterministic models was given by Lloyd (2004), who used different analytic techniques as well as numerical simulations to investigate the departures from deterministic (or mean-field) behaviour of the unforced and seasonally forced SIR models, as a function of the population size. This analysis highlights serious deficiencies of deterministic descriptions of dynamical (long-term) behaviour, especially for seasonally forced models and 'moderate' size ($<10^7$) populations.

Spatial structure is known to be another essential ingredient of the dynamics of epidemic spread. Coarse-grained metapopulation models have been considered to describe phase-locking and decoherence of the observed spatial patterns of infection, as well as their effects on global persistence (Bolker and Grenfell, 1995; Finkenstädt and Grenfell, 1998; Grenfell et al., 2001; Lloyd and May, 1996; Rohani et al., 1999).

The breakdown of the 'homogeneous mixing' hypothesis at a finer spatial scale is yet another cause of departure from mean-field behaviour, namely through the screening of infectives, that has been recognized in individually based cellular automata simulations of the short term dynamics of epidemic bursts (Keeling, 1999; Kleczkowski and Grenfell, 1999; Rhodes and Anderson, 1996a, b). Less well known is the fact that spatial correlations may greatly enhance the stochastic fluctuations.

In this paper, we perform long-term stochastic simulations of individually based cellular automata on small world networks with SIR and SEIR node dynamics. By contrast to spatially structured metapopulation models, based on a coarse-grained distribution of the global population over a few interacting patches (Bolker and Grenfell, 1995; Finkenstädt and Grenfell, 1998; Grenfell et al., 2001; Lloyd and May, 1996; Rohani et al., 1999) in our model the nodes of the network represent individuals. The links are then connections along which the infection spreads. A small world network (Watts and Strogatz, 1998) is an attempt to represent realistically the network of contacts between individuals, where local links predominate but social and geographical mobilities imply a fraction of random connections through which long-range transmission may occur. The spread of infectious disease through a structured population was indeed one of the

applications envisioned by the creators of the small world network model (Watts, 1999). Although for sexually transmitted diseases, other types of contact networks have been shown to be more realistic (Liljeros et al., 2001), for most transmission mechanisms a small world network is the simplest model compatible with the available data incorporating long-range infection.

We start by assessing the effect of network topology on the long-term dynamics of a simple spatially extended model, implementing SIR node dynamics on a cellular automaton living on a square lattice with small world interaction rules (Section 2.2). We find the characteristic long-term dynamics related, in a quantitative fashion, to the structure of the network of contacts. In particular, the increase in spatial correlations (i) enhances the fluctuations around the endemic state; (ii) decreases the effective transmission rate through the screening of infectives and susceptibles; and (iii) increases the period of the incidence oscillations as a result of the lower effective transmission rate. These changes do not follow their mean-field relations revealing the presence of an important spatial structure (Sections 2.3 and 3.2).

In Section 3 we test the model in a more realistic setting, using SEIR node dynamics, a birth rate of $\frac{1}{61}$ year^{-1} and the values reported in the literature (Anderson and May, 1991) for the latency and recovery time of two childhood diseases, measles and pertussis. For measles, the pre-vaccination pattern is accurately reproduced by simple deterministic models with seasonal forcing. This is not the case for pertussis, where it is well known that stochasticity plays an important role. A stochastic version of the standard seasonally forced susceptible-exposed-infective-recovered (SEIR) model generates, for pertussis in the pre-vaccination era, a temporal pattern consistent with the observed dynamics, and for the vaccination era, epidemics with a pronounced 3.5-year period (Rohani et al., 1999) in line with the epidemiological data. These results were obtained by assuming different amplitudes of seasonal forcing for measles and pertussis.

In Section 3.2 we consider the incidence time series given by the cellular automaton when the epidemiological parameters are taken for measles. As with any unforced model, the characteristic annual/biennial cycles of pre-vaccination records cannot be obtained without fine tuning of the model's parameters, infectiousness and probability of long-range infection. However, in the small world region, the amplitudes of the fluctuations are shown to be compatible with incidence records for populations with similar sizes. In order to compare the infectiousness parameter with the values in the literature we have investigated the behaviour of our model in the limit where the links between the nodes are completely random. Apart from providing a way to relate the basic reproductive rate

with the infectiousness parameter in our model, this analysis reveals the mechanism behind recurrent epidemics in unforced spatially extended models, showing how fluctuations decrease along with the spatial correlations as we approach the homogeneously mixed stochastic model.

In Section 3.3 we show how the unforced SEIR model on small world networks produces sustained oscillations with periods and amplitudes compatible with the pertussis data both before and after mass vaccination for realistic values of life expectancy, latency and recovery time. Analysis of the homogeneously mixed limit shows that the infectiousness parameter is also within the reported range for pertussis (Anderson and May, 1991).

Our results for the SIR and SEIR models support the conclusion that, for some purposes, successful modelling of disease spread must take into account the fact that populations are finite and discrete, and must include a realistic representation of the spatial degrees of freedom or, more generally, of the interaction network topology. It also stresses the importance of network connections in real epidemics, an idea that has been acknowledged recently in the context of threshold behaviour (May and Lloyd, 2001; Pastor-Santorras and Vespigniani, 2001a). Finally, it calls for a reassessment of the impact of environmental forcing by studying its effects on a more realistic autonomous model as the one that we propose. In particular, fluctuation enhancement by spatial correlations might remove some of the constraints on the strength of seasonality and avoid fine tuning of seasonal forcing amplitudes.

2. SIR node dynamics on a small world network

2.1. Deterministic and stochastic SIR models

In order to set the notation we start with a brief description of the deterministic and stochastic SIR models.

A community of N (fixed) individuals comprises, at time t, S susceptibles, I infectives in circulation and R recovered or removed (isolated, dead or immune). Constant infection, β, recovery and birth/death rates are assumed. γ is the recovery rate while birth and death rates, μ, are assumed to be equal.

The basic differential equations in terms of the densities, s and i, are

$$\frac{ds}{dt} = -\beta si - \mu s + \mu, \tag{1}$$

$$\frac{di}{dt} = \beta si - (\gamma + \mu)i. \tag{2}$$

Endemic equilibrium occurs at $i_0 = \mu(1/(\gamma + \mu) - 1/\beta)$ and $s_0 = (\gamma + \mu)/\beta$. By linearizing around this point we obtain for the period of the damped oscillations, $T \approx 2\pi/\sqrt{\mu(\beta - \gamma)}$.

In contrast with some SIR models we have considered non-zero birth rates, μ, that will turn out to be crucial to describe the long-term dynamical behaviour of the spatial version of the system (Sections 2.3 and 3).

The stochastic version of the SIR model considers the probability that there are S susceptibles and I infectives and three types of transitions:

$$Pr\{(s,i) \to (s - 1/N, i + 1/N)\} = \beta si \Delta t, \tag{3}$$

$$Pr\{(s,i) \to (s, i - 1/N)\} = \gamma i \Delta t + \mu i \Delta t, \tag{4}$$

$$Pr\{(s,i) \to (s + 1/N, i)\} = \mu \Delta t - \mu s \Delta t. \tag{5}$$

The stochastic change in the number of susceptibles in time Δt is the sum of the loss due to infection, Poisson distributed with mean $N\beta si \Delta t$, or death, also Poisson distributed with mean $N\mu s \Delta t$, and the gain due to the arrival of new susceptibles, Poisson distributed with mean $N\mu \Delta t$. Similarly, the stochastic change in the number of infectives is the sum of a Poisson distributed gain due to infection, with mean $N\beta si \Delta t$, and a loss from death or recovery Poisson distributed with mean $N(\gamma + \mu)i \Delta t$.

The endemic equilibrium is the same as that of the underlying deterministic model. The equations for the stochastic changes in s and i may be linearized about the endemic equilibrium values and the variance of the fluctuations is easily obtained $\sigma_s^2 = 1/s_0 + (1 - s_0)/i_0$ and $\sigma_i^2 = 1/(i_0(1 - s_0)) + (s_0(1 - s_0))/i_0^2$.

We note that in this regime the fluctuations about the endemic state scale as the square root of the system size. These fluctuations exhibit a temporal structure modulated by the underlying deterministic dynamics and thus oscillate (on average) with the period of the damped oscillations of the corresponding deterministic model. The amplitude of these fluctuations is, however, small and the size of the recurrent epidemic peaks is often underestimated by a homogeneously mixed stochastic model.

2.2. Stochastic SIR model on a small world network

The SIR model is easily generalized to an epidemic that takes place on a network. As for models of epidemic spread on regular lattices (Grassberger, 1983), the model may be mapped onto percolation on the same network (Moore and Newmann, 2000a). The percolation transition corresponds to the epidemic threshold, above which an epidemic outbreak is possible (i.e. one that infects a non-zero fraction of the population, in the limit of large populations) and the

size of the percolating cluster above this transition corresponds to the size of the epidemic.

In recent works, the role of the network topology for SIS and SIR models with zero birth rate has been considered in the calculation of epidemic thresholds (May and Lloyd, 2001; Moore and Newmann, 2000a, b; Pastor-Santorras and Vespigniani, 2001a) the stationary properties of the endemic state (Pastor-Santorras and Vespigniani, 2001b), and in the short-term dynamics of epidemic bursts (Keeling, 1999; Kleczkowski and Grenfell, 1999, Rhodes and Anderson, 1996). By contrast, the effects of network topology on the long-term dynamics of epidemic spread remain poorly understood.

We shall consider a small world contact network. This type of networks have topological properties that interpolate between lattices and random graphs, and were first proposed by Watts and Strogatz (1998) as realistic models of social networks. A fraction of the links is randomized by connecting nodes, with probability p, with any other node on the lattice; the number of links is preserved by removing a lattice link when a random one is established. The interpolation is non linear: for a range of p the network exhibits small world behaviour, where a predominantly local neighbourhood (as in lattices) coexists with a short average path length (as in random graphs). A small world network over a regular network is defined, in a statistical sense, by the small world parameter p. Another useful quantity to characterize it is the clustering coefficient C, that measures the locality of the network. The clustering coefficient is defined as the averaged fraction of all the possible links between neighbours of a given node that are actually present in the network. Analysis of real networks (Dorogotsev and Mendes, 2003) reveals the existence of small worlds in many interaction networks, including networks of social contacts.

In order to take into account spatial variations ignored in homogeneously mixed stochastic models, we consider a cellular automaton (CA) on a square lattice of size $N = L^2$. The (random) variables at each site may take one of three values: S, I or R. The lattice is full, $N = S + I + R$. We consider local interactions with $k = 4n$ neighbouring sites on the square lattice (first neighbours along the N, S, E and W directions, first neighbours along the NE, NW, SW and SE directions, second neighbours along N, S, E and W, and so on), as well as random long-range interactions, with a small world probability, p, with any other site on the lattice. The total rate of infection β is the sum of the local and long-range rates of infection, given in terms of the small world parameter by $\beta(1 - p)$ and βp, respectively. We have used different types of boundary conditions (absorbing and helicoidal) and checked that the results do not depend on them. The results depend quantitatively, but not qualitatively, on the number k of

neighbouring sites, provided that k is much smaller than the size of the lattice.

Birth, death and infection occur stochastically, with fixed rates (μ, μ, β) while recovery, characterised by a disease dependent period, is deterministic (after $\tau_i = 1/\gamma$ time steps). This disease-dependent period sets the time scale of the model. At each Monte Carlo step, N random site updates are performed following a standard algorithm. One type of event, long and short-range infection, death and birth, is chosen with the appropriate rate (βp, $\beta(1 - p)$, μ, μ, respectively) and then proceeds as follows. For infection events, one site is chosen at random; if the site is in the infective, I, or recovered, R, states no action is taken. If the site is in the susceptible state, S, one other site (one of its $k = 12$ nearest neighbours for local infection or any other site on the lattice for long-range infection) is chosen at random; the first site becomes infected iff the second site is in the infective state, I. For a death event, a site is chosen at random and death occurs regardless; the state is then changed into the removed or recovered state, R. Finally, for birth events a recovered site, R, is searched at random until it is found; then it is changed into the susceptible, S state.

To account for the deterministic recovery, counters are assigned to all sites and are set to -1; the counters of the infective sites, I, are updated at each time step. After $\tau_i = 1/\gamma$ MC steps (recovery time) the infectives recover, that is the sites in the I state change into the R state.

2.3. Results for the stochastic SIR model on a small world network

Apart from the network parameter p that determines the fraction of long distance infection, the spatial SIR model depends only on three additional parameters. Two of them are the infectious period and life expectancy, and the other, β, the infectiousness of the disease. The first two are determined from medical and demographic data (Anderson and May, 1991) and we show that p and β may be obtained from fits to epidemiological data. Thus the model provides quantitative information on the structure of the network of contacts underlying the spread of a particular disease.

In Fig. 1 we summarize the results for the persistence (fraction of the simulations surviving a given number of time steps) as a function of the small world parameter p for a population of $N = 250,000$. The other model parameters are kept fixed at $\mu = 0.0006\,\text{day}^{-1}$, $\gamma = 0.0625 = \frac{1}{16}\,\text{day}^{-1}$ and $\beta = 0.66\,\text{day}^{-1}$. The persistence is almost zero at low p, and approaches one over a narrow range of p, for a population of this size. The transition between extinction and persistence is a percolation transition. The epidemic persists in finite populations as a result of the finite birth rate that allows the renewal of susceptibles.
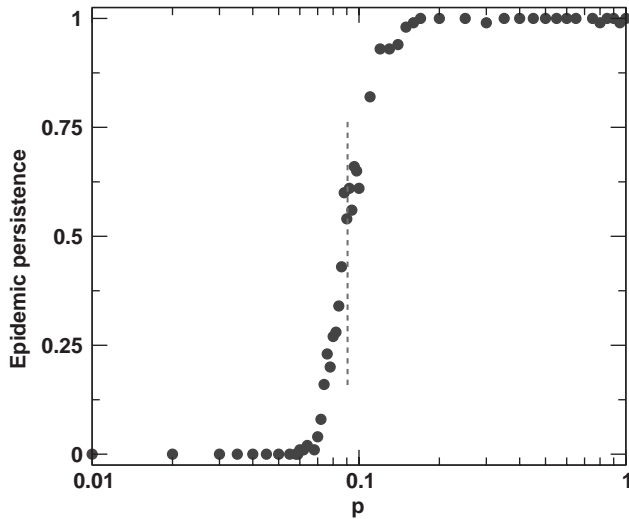
Fig. 1. Epidemic persistence transition. Fraction of the simulations that survive for 20,000 days as a function of the small world parameter p, for a discrete SIR model. Infection occurs between connected sites. Each site has 12 connections, an average fraction $1 - p$ of which are neighbours on the lattice; the remaining fraction p is chosen randomly at each time step. The persistence is almost zero, at low p ($p < 0.07$) and approaches one over a narrow range of p close to 0.09, for a population of 250,000. The abrupt change in persistence is a percolation transition on the small world network.

On regular lattices the transitions are isotropic percolation transitions if a site cannot be re-infected and directed percolation if re-infection (through birth of susceptibles, mutation of infectious agents, etc.) occurs (Dammer and Hinrichsen, 2003). In the presence of random long-range interactions on the complex network the transitions become mean-field with an anomalous asymptotic region (Hastings, 2003). In addition, finite size effects broaden the transition region considerably. We note that by contrast with atomic systems, whose sizes are effectively infinite, finite size effects cannot be ignored in this context. A detailed study of these effects, as well as the dependence of the thresholds on relevant epidemiological parameters, will be published elsewhere.

In Fig. 2 we have plotted the clustering coefficient (Watts and Strogatz, 1998) of the underlying small world network for the parameters of Fig. 1. The persistence and the root mean square amplitude of the epidemic peaks of the SIR model are also shown. When the clustering is large (as in lattices) the fluctuations are large and stochastic extinction occurs. When $p = 1$ the fluctuations are small (as in homogeneously mixed stochastic models) and the epidemic persists. The persistence transition occurs in the region of intermediate clustering, i.e., at the edge of the small world regime where the fluctuations are sufficiently small for stochastic extinction to become rare.

The effective transmission rate, $\beta_{eff} N$, the average number of new infectives per time step divided by the product of the instantaneous densities of susceptibles
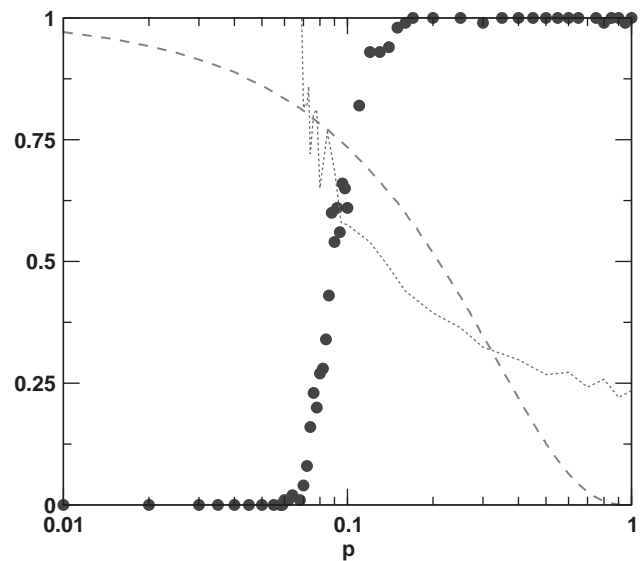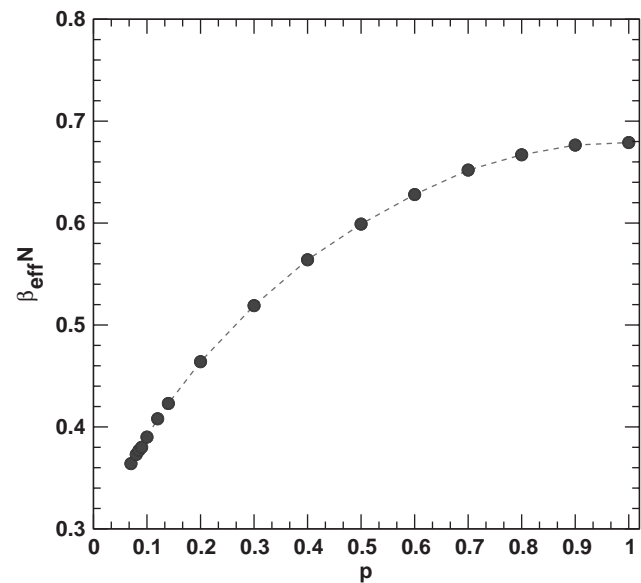

Fig. 2. Small world parameters and the epidemic persistence transition. Clustering coefficient (dashed line) for the underlying small world network. The fraction of the simulations that survive for 20,000 days (circles), and the root mean square amplitude of the epidemic peaks (dotted line) is also shown. The clustering coefficient and the root mean square amplitude of the peaks were measured relative to the lattice values. The persistence transition occurs at the edge of the small world regime.

Fig. 3. Effective transmission rate vs the network parameter, p. The effective transmission rate, $\beta_{eff} N$, is calculated as the average number of new infectives per time step divided by the product of the instantaneous densities of susceptibles and infectives. The drastic reduction in $\beta_{eff} N$ is due to the clustering of infectives and susceptibles as p decreases and the spatial correlations increase. The model and the parameters are the same as in Fig. 1.

and infectives, is shown in Fig. 3. These rates differ from those reported by Kleczkowski and Grenfell (1999) for simulations spanning a single epidemic wave, in two ways. First, we focus on the long-term dynamical regime

and exclude from the analysis the transient corresponding to the initial dynamical regime. In addition, the effective transmission rates are calculated during the simulation runs while those reported by Kleczkowski and Grenfell (1999) were obtained by fitting simulated time series to approximate mean-field solutions.

The significant variation of the effective transmission rate with p is due to the clustering of infectives and susceptibles and has to be taken into account in fittings to effective mean-field models. This clustering, and spatial correlations in general, also have drastic consequences on the amplitude and on the period of the incidence oscillations. The typical values of these quantities for a given time series can be used for model fitting and testing. We will return to this point in the next section.

3. SEIR node dynamics on a small world network

3.1. Stochastic SEIR model on a small world network

In this section, we show that epidemic models on small world networks provide a natural basis for the description of recurrent epidemic dynamics, by reporting realistic modelling of two childhood diseases, measles and pertussis. We have obtained, using the SEIR model, sustained oscillations with periods and amplitudes compatible with the data for realistic values of the model parameters. In recent works (Johansen, 1996; Kuperman and Abramson, 2001) a relation was suggested between spatial structure and the onset of recurrent epidemics, but in both models the periods of the incidence oscillations are of the order of the time elapsed between infection and loss of immunity, and thus the conclusions are not relevant for immune for life diseases. In particular, in Kuperman and Abramson (2001), the homogeneously mixed model exhibits oscillatory behaviour which is destroyed by spatial correlations through loss of global synchrony, so that the reported effect is in a sense the opposite of what we find here.

The spatial SEIR model is similar to the spatial SIR model, but the recovery time is split into latent and infectious periods. During the latent period an S has become infected but yet cannot infect another susceptible. The rules are as in the spatial SIR model with the following modifications. Infection: S is infected iff the second site is an infective in the infectious period, I; in this case S is changed into the exposed E state. The counters of the exposed and infective sites are updated. After τ_l steps (latency) the exposed sites, E, change into the infective state, I; the infectious period lasts for an additional τ_i steps. Recovery is deterministic and occurs after $\tau_l + \tau_i$ steps.

We have taken $\mu = \frac{1}{61}\,\mathrm{year}^{-1}$ for the birth rate and a population size of $N = 10^6$ in all the simulations. For measles, we have set $\tau_i = 8$ days, $\tau_l = 6$ days and $\beta = 2.4\,\mathrm{day}^{-1}$ for the homogeneously mixed model, $p = 1$, and $\beta = 4.75\,\mathrm{day}^{-1}$ for the network model with $p = 0.2$. For pertussis we set $\tau_i = 18$ days, $\tau_l = 8$ days and $\beta = 1.5\,\mathrm{day}^{-1}$ for the homogeneously mixed model, $p = 1$, and $\beta = 4.0\,\mathrm{day}^{-1}$ for the network model with $p = 0.2$. Given the length and variability of the infectious period of pertussis, deterministic recovery was changed for Poisson recovery. The end of the latency period was kept deterministic.

3.2. Results for SEIR dynamics simulations of measles

We obtained new infectives time series on $N = 1000 \times 1000$ lattices. The time series for measles in homogeneously mixed populations, $p = 1$, exhibit sustained fluctuations (Fig. 4a) with an average period of two years. However, the amplitude of the fluctuations is underestimated when compared with the incidence oscillations of measles in Birmingham (From data
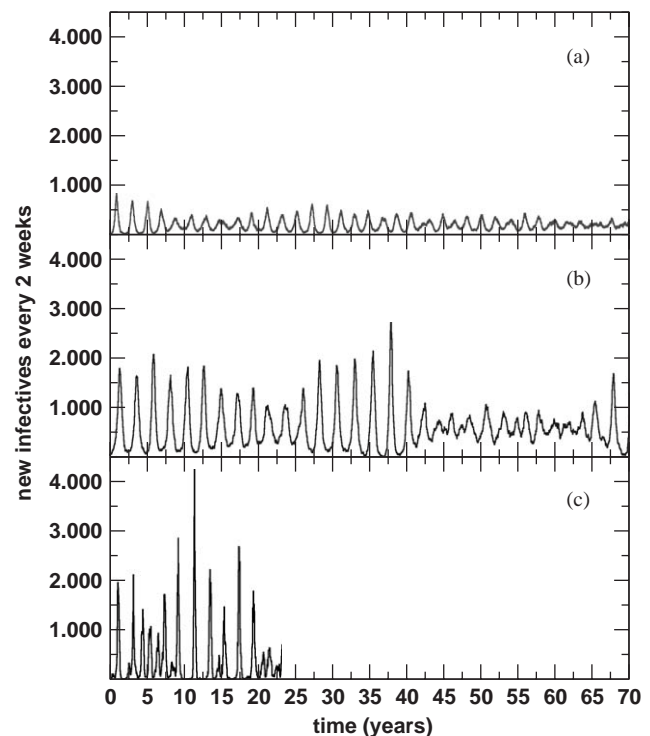

Fig. 4. New infectives time series for homogeneously mixed and spatially structured populations. Number of new infectives every 2 weeks, from SEIR simulations on $N = 1000 \times 1000$ lattices. (a) The results for measles in a homogeneously mixed population, $p = 1$, and transmission rate $\beta = 2.4\,\mathrm{day}^{-1}$, exhibit sustained fluctuations with an average period of two years. The amplitude of the fluctuations is underestimated when compared with the amplitude of measles incidence peaks from Birmingham (c). (b) The results for measles on a network with $p = 0.2$ and $\beta = 4.75\,\mathrm{day}^{-1}$ exhibit an average period close to two years but the amplitude of the incidence oscillations is larger in line with the real data (c).

at http://www.zoo.cam.ac.uk/zoostaff/grenfell/measles.htm) (Fig. 4c) with a similar population size (about 10^6 during the reported period).

As discussed in the previous section we found that the fluctuations are enhanced as a result of clustering when p decreases. Consequently, in a range of p around the persistence transition we can account for the amplitude of the incidence peaks, in sharp contrast with homogeneously mixed stochastic models. Conversely, reliable values of the incidence peaks become in view of this a measure of p, leaving only β to be fitted to experimental data.

In Fig. 4b we plot new infectives time series, for SEIR simulations on a network with $p = 0.2$, and β corresponding to incidence oscillations with an average period of 2 years (other parameters as in Fig. 4a). The amplitude of the incidence peaks is shown to increase significantly, in line with the real data. As a further check we report the average age at infection for both models. We found that while the homogeneously mixed model underestimates the average age at infection (~ 3 years) the small world model, with $p = 0.2$, increases it by 20% in line with epidemiological data. Since the incidence oscillations have similar periods in both models this result provides additional support of the network model.

We remark that the effect of spatial correlations on the period is striking. We found that the period increases by up to a factor of two as p decreases, as a consequence of the reduced effective transmission rate, suggesting that the contact network structure may play a role in the triennial epidemic cycles observed in the pre-vaccination measles records of cities such as Copenhagen and Baltimore (Bolker and Grenfell, 1995). However, spatial correlations have further implications, beyond the screening of infectives and its consequences. We have shown that stochastic fluctuations are significantly enhanced, and that, as the homogeneous mixing relations breakdown, the period and the average age at infection change independently in this model.

Despite the fact that, for measles, seasonality cannot be ignored, and that pre-vaccination incidence records are well reproduced by simpler deterministic models with seasonal forcing, the reported effects of spatial correlations should also be taken into account. We expect that adding seasonality to our model will produce time series showing robust annual/binneal peaks with the observed incidences for a wide range of forcing amplitudes.

3.3. Results for SEIR dynamics simulations of pertussis

While for measles seasonal forcing is the basic ingredient to explain pre-vaccination long-term dynamics, this is not the case for pertussis, where stochasticity plays an important role.

We have obtained, using SEIR simulations, new infectives time series on $N = 1000 \times 1000$ lattices for pertussis. Given that the infectious period of pertussis varies from 14 to 21 days we modelled the recovery of pertussis stochastically. In Fig. 5a we plot new infectives time series for pertussis on the same network as measles ($p = 0.2$), with $\beta = 4.0\,\mathrm{day}^{-1}$ corresponding to pre-vaccination incidence oscillations with a broad 2.5 year period. The root mean square amplitude of the incidence peaks is compatible with reported epidemiological data (Rohani et al., 1999). It is obvious from Figs. 4 and 5 that pertussis exhibits epidemic peaks that are much noisier than those of measles. In our model, this is due in part to the stochastic recovery process. However, the effects of spatial correlations, that are significant close to the epidemic persistence transition, are much less evident for pertussis. This is confirmed by the results for pertussis of the homogeneously mixed SEIR model, $p = 1$, that are plotted in Fig. 5b. This time series exhibits sustained fluctuations (Fig. 5b) with an amplitude that is similar to that of the network model ($p = 0.2$), in marked contrast with the results for measles (Fig. 4) for the same contact network. Therefore, the importance of the spatial correlations depends also on the particular disease.
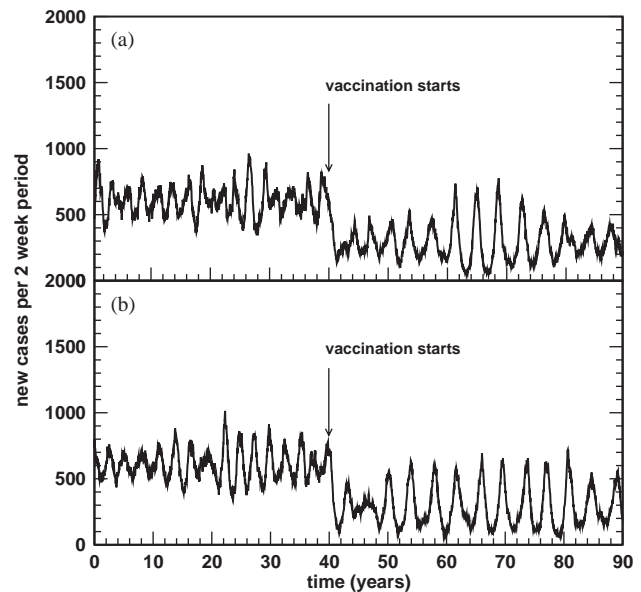

Fig. 5. New infectives time series for homogeneously mixed and spatially structured populations. Number of new infectives every 2 weeks, from SEIR simulations on $N = 1000 \times 1000$ lattices. (a) The results for pertussis on a network with $p = 0.2$ and $\beta = 4.0\,\mathrm{day}^{-1}$. The time series is noisier than that for measles on the same network. After mass vaccination both the period of the incidence oscillations and the spatial coherence increase. (b) The results for pertussis on a homogeneously mixed population, $p = 1$, and transmission rate $\beta = 1.5\,\mathrm{day}^{-1}$, exhibit sustained fluctuations with the same average period. The behaviour of pertussis in the pre and post-vaccination periods is similar to that of the network model indicating that stochastic effects dominate the behaviour of these time series.

Finally, in Fig. 5 we have plotted new infective time series for pertussis after mass vaccination. We assumed a vaccination coverage of 80% with 70% efficacy and modelled it by reducing the birth rate to one-half of its value in the pre-vaccination era. It is clear that the unforced spatial SEIR model is capable of describing the increase in the period of the recurrent epidemic peaks reported after mass vaccination while increasing their spatial coherence, in agreement with available data (Rohani et al., 1999). In our model, this increased coherence is due to the loss of stability of the endemic equilibrium.

These results show that spatially extended SEIR models on small world networks exhibit sustained oscillations, that differ from the stochastic fluctuations of homogeneously mixed stochastic models, under various conditions relevant to the description of childhood diseases. In particular, both the observed periods and the spatial coherence of the epidemic peaks of pertussis, before and after mass vaccination, are described by this spatially extended unforced model.

4. Discussion and conclusions

We performed long-term stochastic simulations of individually based cellular automata on small world networks with SIR and SEIR node dynamics. This model has the recognized basic ingredients for realistic modelling, namely stochasticity, a discrete and reasonably sized finite population, epidemiological parameters as given in the literature for two childhood diseases, and spatial structure given by a plausible contact network. Indeed, the small world network has the path length and clustering properties shared by most real networks and its Poisson degree distribution, where the node connectivity is sharply peaked about the mean, is a reasonable representation of the social contacts among school children.

As expected, the long-term dynamics is dominated by stochastic fluctuations around mean-field behaviour. However, when the network's clustering coefficient is in the small world region, i.e., in the range of typical values measured for social networks, the amplitude of the stochastic fluctuations is enhanced significantly by spatial correlations. In particular, away from the boundary of the small world region, where the clustering coefficient is high and the interactions are predominantly local, fluctuations lead to extinction on short time-scales, for other parameters above the endemic threshold of the homogeneously mixed model. For the remaining range of the clustering coefficient, epidemics persist for times that approach those of homogeneously mixed populations providing suitable models to investigate the effects of spatial correlations on the long-term dynamics of epidemic spread.

This has three major consequences. First, when spatial structure is taken into account in stochastic models the size of the population for which the stochastic and deterministic descriptions agree is larger than when homogeneous mixing is assumed, due to the enhancement of fluctuations by the spatial correlations. Second, for small world networks, the persistence threshold corresponds to the region where the clustering coefficient starts to decrease, along with the relative fluctuations. Third, time series of the (unforced) model provide patterns of recurrent epidemics with slightly irregular periods and realistic amplitudes, suggesting that stochastic models together with spatial correlations are sufficient to describe the long-term dynamics when seasonal forcing is weak or absent.

Annual and biennial regular temporal patterns are the signature of seasonally forced models, but these may also exhibit different dynamics, such as triennial cycles and chaotic behaviour. Stochastic effects on seasonally forced models can also produce slightly irregular, realistic, time series. Then, how can the basic mechanism(s) of recurrent epidemics be determined from the case report data ? Our model reduces to the mean-field stochastic model for $p = 1$ and large N, but in the range of epidemiologically relevant population sizes, finite size effects are important and spatial correlations cannot be ignored. The epidemic peaks obtained from our model scale as N^a, $\frac{1}{2} \leqslant a < 1$, $a - \frac{1}{2}$ being a measure of the effect of spatial correlations. By contrast, seasonally forced peaks scale as N. For a given disease and a given seasonality, the peaks over several cities must scale with the population N.

The different scaling forms of epidemic peaks predicted by the two models could be used, in principle, to discriminate the underlying mechanism of the incidence oscillations characteristic of a given class of diseases. Linear fits for measles in England and Wales do rather well but two-parameter power law fits do almost as well with $a \approx \frac{3}{4}$. However the importance of seasonal forcing for this example is unquestionable, and a sublinear fit may be the result of a de-phasing effect.

In conclusion, we have shown that fine grained discrete models based on contact structure are realistic autonomous models, that are computationally feasible for relevant population sizes. In the small world regime, they exhibit sustained fluctuations with well-defined period and amplitudes within the observed range. These quantities may be used to fit the model's free parameters, p and β. The fact that this can be done with satisfactory quantitative agreement for the simplest version of the model puts it on the level of the traditional deterministic and stochastic models as a basis for realistic modelling. The impact of other factors, such as seasonal forcing, age structure and spatial heterogeneity, should be reassessed based on this.

Acknowledgements

References

Anderson, R.M., May, R.M., 1986. The invasion, persistence and spread of infectious diseases within animal and plant communities. Philos. Trans. R. Soc. London Ser. B 314, 533–570.

Anderson, R.M., May, R.M., 1991. Infectious Diseases of Humans, Dynamics and Control. Oxford University Press, Oxford.

Aparicio, J.P., Solari, H.G., 2001. Sustained oscillations in stochastic systems. Math. Biosci. 169, 15–25.

Aron, J.L., Schwartz, I.B., 1984. Seasonality and period-doubling bifurcations in an epidemic model. J. Theor. Biol. 110, 665–679.

Bailey, N.T.J., 1975. The Mathematical Theory of Infectious Diseases, second ed. Charles Griffin, London.

Bartlett, M.S., 1957. Measles periodicity and community size. J. R. Stat. Soc. Ser. A 120, 48–70.

Bolker, B., 1993. Chaos and complexity in measles models—a comparative numerical study. IMA J. Math. Appl. Med. 10, 83–95.

Bolker, B., Grenfell, B.T., 1995. Space, persistence and dynamics of measles epidemics. Philos. Trans. R. Soc. London Ser. B 348, 309–320.

Dammer, S.M., Hinrichsen, H., 2003. Epidemic spreading with immunization and mutations. Phys. Rev. E 68, 016114.

Dietz, K., 1976. Lect. Notes Biomath. 11, 1–15.

Dorogotsev, S.N., Mendes, J.F., 2003. Evolution of Networks. Oxford University Press, Oxford.

Earn, D.J.D., Rohani, P., Bolker, B.M., Grenfell, B.T., 2000. A simple model for complex dynamical transitions in epidemics. Science 287, 667–670.

Finkenstädt, B., Grenfell, B., 1998. Empirical determinants of measles metapopulation dynamics in England and Wales. Proc. R. Soc. London Ser. B 265, 211–220.

Grassberger, P., 1983. On the critical behaviour of the general epidemic process and dynamical percolation. Math. Biosci. 63, 157–172.

Grenfell, B.T., Bjornstad, O.N., Kappey, J., 2001. Travelling waves and spatial hierarquies in measles epidemics. Nature 414, 716–723.

Hastings, M.B., 2003. Mean-field and anomalous behaviour on a small world network. Phys. Rev. Lett. 91, 098701.

Hethcote, H.W., 2000. The mathematics of infectious diseases. SIAM Rev. 42, 599–653.

Johansen, A., 1996. A simple model of recurrent epidemics. J. Theor. Biol. 178, 45–51.

Keeling, M.J., 1999. The effects of local spatial structure on epidemiological invasions. Proc. R. Soc. London Ser. B 266, 859–867.

Keeling, M.J., Grenfell, B.T., 1997. Disease extinction and community size: modeling the persistence of measles. Science 275, 65–67.

Keeling, M.J., Grenfell, B.T., 2002. Understanding the persistence of measles: reconciling theory simulation and observation. Proc. R. Soc. London Ser. B 269, 335–343.

Kleczkowski, A., Grenfell, B.T., 1999. Mean field type of equations for spread of epidemics: the small world model. Physica A 274, 355–360.

Kuperman, M., Abramson, G., 2001. Small world effect in an epidemiological model. Phys. Rev. Lett. 86, 2909–2912.

Liljeros, F., Edling, C.R., Amaral, L.A.N., Stanley, E., Åberg, Y., 2001. The web of human sexual contacts. Nature 411, 907–908.

Lloyd, A.L., 2004. Estimating variability in models for recurrent epidemics: assessing the use of moment closure techniques. Theor. Pop. Biol. 65, 49–65.

Lloyd, A.L., May, R.M., 1996. Spatial heterogeneity in epidemic models. J. Theor. Biol. 179, 1–11.

May, R.M., Lloyd, A.L., 2001. Infection dynamics on scale free networks. Phys. Rev. E 64, 066112.

Moore, C., Newmann, M.E.J., 2000a. Epidemics and percolation in small world networks. Phys. Rev. E 61, 5678–5682.

Moore, C., Newmann, M.E.J., 2000b. Exact solution of site and bond percolation on small world networks. Phys. Rev. E 62, 7059–7064.

Murray, J.D., 2003. Mathematical Biology, II: Spatial Models and Biomedical Applications. Springer, Heidelberg.

Nåsell, I., 1999. On the time to extinction in recurrent epidemics. J. R. Stat. Soc. Ser. B 69, 309–330.

Pastor-Santorras, R., Vespigniani, A., 2001a. Epidemic spreading in scale free networks. Phys. Rev. Lett. 86, 3200–3203.

Pastor-Santorras, R., Vespigniani, A., 2001b. Epidemic dynamics and endemic states in complex networks. Phys. Rev. E 63, 066117.

Rhodes, C.J., Anderson, R.M., 1996a. Persistence and dynamics in lattice models of epidemic spread. J. Theor. Biol. 180, 125–133.

Rhodes, C.J., Anderson, R.M., 1996b. Power laws governing epidemics in small populations. Nature 381, 600–602.

Rohani, P., Earn, D.J.D., Grenfell, B.T., 1999. Opposite patterns of synchrony in sympatric disease metapopulations. Science 286, 968–971.

Rohani, P., Keeling, M., Grenfell, B., 2002. The interplay between determinism and stochasticity in childhood diseases. Am. Nat. 159, 469–481.

Watts, D.J., 1999. Small Worlds. Princeton University Press, Princeton, NJ.

Watts, D.J., Strogatz, S.H., 1998. Collective dynamics of 'small-world' networks. Nature 393, 440–442.